Catalysis Communications 108 (2018) 1–6

Contents lists available at ScienceDirect

Catalysis Communications

journal homepage: www.elsevier.com/locate/catcom

Short communication

Fine tuning the enantioselectivity and substrate specificity of alcohol dehydrogenase from *Kluyveromyces polysporus* by single residue at 237

Yue Wang[a], Wei Dai[a], Yongmei Liu[b], Zhongwei Zhang[a], Jieyu Zhou[a], Guochao Xu[a,*], Ye Ni[a,*]

[a] The Key Laboratory of Industrial Biotechnology, Ministry of Education, School of Biotechnology, Jiangnan University, Wuxi 214122, Jiangsu, China
[b] School of Pharmacy, Taizhou Polytechnic College, Taizhou 225300, Jiangsu, China

ARTICLE INFO

Keywords:
Saturation mutagenesis
Enantioselectivity
Diaryl alcohols
S237
*Kp*ADH

ABSTRACT

Here, S237 was identified to be important in fine tuning the substrate specificity and enantioselectivity of alcohol dehydrogenase from *Kluyveromyces polysporus* (*Kp*ADH). In the reduction of a diaryl ketone, (4-chlorophenyl)-(pyridin-2-yl)-methanone (**1a**), the highest and lowest enantioselectivity of 96.1% and 27.0% *e.e.* (*R*) were obtained with S237A and S237C. Kinetic parameters analysis revealed that S237G, S237A, S237H and S237D displayed improved k_{cat}/K_m toward **1a**. Various prochiral ketones, including acetophenone, 4-chloroacetophenone and ethyl 2-oxo-4-phenylbutyrate could be asymmetrically reduced by S237C, S237G and S237E with > 99% *e.e.* This study provides guidance for the application of *Kp*ADH in the preparation of chiral secondary alcohols.

1. Introduction

Alcohol dehydrogenases are arising as one of the most promising catalysts in the synthesis of chiral compounds, due to their 100% theoretical yield, high selectivity, mild condition and environmental benignancy [1–3]. Various naturally evolved or tailor-made alcohol dehydrogenases have been successfully applied in pharmaceuticals, agrochemicals and liquid materials [4–6]. However, their complex and sophisticated structures often result in narrow substrate specificity [7–9]. It is of increasing interest to identify novel alcohol dehydrogenases with activity toward substrates with diverse substituents [10–12].

Diaryl ketones could be reduced into diaryl alcohols which are key building blocks of antihistamine, antiepileptic, antibechic and antidepressant pharmaceuticals [13,14], and are widely accepted as “hard-to-reduce” substrates for alcohol dehydrogenases because of their high steric hindrance, inertness and similarity of two aromatic substituents [5,11]. Few alcohol dehydrogenases have been identified with activity toward diaryl ketones [15–18]. SSCR from *Sporobolomyces salmonicolor* could reduce (4-chlorophenyl)-phenylmethanone at 10 mM with 62% conversion rate and 88% *e.e.* (*R*) [17]. Commercial ketoreductases have been evaluated for asymmetric reduction of diaryl ketones, and KRED124 could reduce (4-chlorophenyl)-(pyridin-2-yl)-methanone (**1a**) into (*R*)-(4-phenyl)-(pyridin-2-yl)-methanol (**1b**), a vital intermediate of anti-allergic drug Betahistine. **1a** (10 $g{\cdot}L^{-1}$) was reduced with 98% conversion rate and 94% *e.e.* under 1 $g{\cdot}L^{-1}$ $NADP^+$ and 2 $g{\cdot}L^{-1}$ purified KRED124 [16]. As a result, asymmetric reduction of diaryl ketones is still challenging, and the identification of key residues in discriminating two bulky aromatic groups of **1a** is of special interests in prompting the biocatalytic preparation of chiral diaryl alcohols.

Alcohol dehydrogenase *Kp*ADH was identified from *Kluyveromyces polysporus* by genome mining [19], and was efficient in preparation of diaryl secondary alcohols, as much as 100 mM **1a** (21.7 $g{\cdot}L^{-1}$) could be completely converted into (*R*)-**1b** with 82% *e.e.* The stable performance of *Kp*ADH even at high substrate loading indicates that *Kp*ADH is promising in the synthesis of chiral secondary alcohols. In this study, *Kp*ADH was engineered by site-directed mutagenesis and a vital residue was identified in tuning the substrate specificity and enantioselectivity. The application potential of *Kp*ADH variants in the preparation of chiral secondary alcohols was also evaluated.

2. Experimental

2.1. Construction and activity assay of KpADH variants

Site-directed mutagenesis was performed employing whole plasmid PCR with pET28a-*kpadh* as template and primers listed in Table S1. The resultant PCR products were digested by addition of 1.0 μL QuickCut™ *Dpn* I at 37 °C for 1 h to remove the parental plasmids and transformed into *E. coli* BL21(DE3). *Kp*ADH coding genes were induced with 0.2 mM IPTG at 25 °C and 180 rpm for 6 h. Cells were harvested, re-suspended with Buffer A, and disrupted by high pressure homogenization at

* Corresponding authors.
E-mail addresses: guochaoxu@jiangnan.edu.cn (G. Xu), yni@jiangnan.edu.cn (Y. Ni).

https://doi.org/10.1016/j.catcom.2018.01.012
Received 11 November 2017; Received in revised form 11 January 2018; Accepted 12 January 2018
Available online 13 January 2018

600–800 bar (AH-BASICII, ATS Engineering Inc.). Supernatant was isolated by centrifugation at 8000 × *g* and 4 °C for 30 min, filtered and loaded on the HisTrap FF nickel column using AKTA Avant System (GE Healthcare). All the *Kp*ADH variants were gradient eluted and purified to homogeneity [21]. Activity assay toward 1.0 mM **1a**, acetophenone (**2a**), 4′-chloroacetophenone (**3a**), ethyl 4-chloroacetoacetate (**4a**), ethyl benzoylformate (**5a**), ethyl 2-oxo-4-phenylbutyrate (**6a**), 1-(pyridin-2′-yl)-phenylmethanone (**7a**), 1-(4′-fluorophenyl)-phenylmethanone (**8a**), 2-chloro-1-(4′-chlorophenyl)-ethanone (**9a**) and 1-(4′-chlorophenyl)-phenylmethanone (**10a**) was performed as previously reported in triplicate [19].

2.2. Bioconversion and determination of enantioselectivity

Bioconversion was conducted with 20 mM **1a–10a**, 20 U·mL^{-1} *Kp*ADH variants, 40 mM isopropanol in PBS buffer (pH 7.0, 100 mM) in total volume of 2 mL at 30 °C and 180 rpm overnight. Then, 1 mL of the reaction mixture was withdrawn and extracted with ethyl acetate. The organic phase was isolated by centrifugation and dried over anhydrous $MgSO_4$. The conversion rate and enantioselectivity of the products were analyzed as described in supporting information.

3. Results and discussion

3.1. Analysis and identification of hot spots of KpADH

For further application of *Kp*ADH in preparation of chiral alcohols, semi-rational mutagenesis was performed. Firstly, the model of *Kp*ADH was built by homology modeling with crystal structure of Gre2p from yeast (PDB No. 4PVD) as template [20]. According to the Ramachandran chart (Fig. S1), 98.55% residues were located in the maximum allowable region, indicating this model was acceptable. Substrate binding pocket was identified by searching the cave and consisted of residues F86, Y127, M131, P133, Q136, F161, C165, S196, F197, E214, S237 and Q238 (Fig. 1A). All these residues were site-directly mutated into alanine to evaluate their influence on the activity of *Kp*ADH. As shown in Fig. 1B, relative activities of variants Q136A, F161A, F197A and Q238A toward **1a** were < 20% of wild-type *Kp*ADH (^{WT}*Kp*ADH). Mutation of E214 and S237 resulted in improved activity of 125.6% and 232.4% respectively. Considering the highest activity of variant S237A, saturation mutagenesis was performed at S237 to elucidate its detailed roles. All nineteen variants were constructed and confirmed by SDS-PAGE (Fig. S2), and the enzymatic properties of purified enzyme were investigated, including specific activity, enantioselectivity, kinetic parameters and substrate specificity.

3.2. Activity and enantioselectivity analysis of KpADH variants mutated at S237

The specific reductive and oxidative activities of purified *Kp*ADH toward **1a** and isopropanol were 11.4 and 18.3 U mg^{-1} respectively. Substrate **1a** could be reduced into (*R*)-**1b** with *e.e.* of 82% by *Kp*ADH obeying anti-Prelog priority. The specific reductive activities of S237A, S237G, S237D, S237 W and S237E were 23.2, 22.7, 18.0, 12.8 and 12.7 U mg^{-1} respectively, which were 2.04-, 1.99-, 1.58-, 1.12- and 1.11-fold of that of ^{WT}*Kp*ADH (Fig. 2). Mutation of serine at 237 into leucine (S237L), valine (S237V), isoleucine (S237I) and threonine (S237T) resulted in severely decreased specific activities of 5.21, 2.93, 2.91 and 1.71 U·mg^{-1}. The oxidative activity of *Kp*ADH was significantly influenced by mutation of Ser237, and only S237A exhibited higher specific oxidative activity of 25.8 U·mg^{-1}, which was 1.41-fold of ^{WT}*Kp*ADH (Fig. 2). < 1.0 U·mg^{-1} of oxidative activity was detected for S237H, S237T and S237V. Although properties of threonine are supposed to be similar to serine, the reductive and oxidative activities of S237T were much lower than ^{WT}*Kp*ADH.

Enantioselectivity analysis revealed that enantioselectivity of *Kp*ADH could be finely manipulated by mutation of S237. Mutation of serine at 237 into alanine rendered *Kp*ADH the highest selectivity in discriminating the chlorophenyl and pyridin-2-yl groups, with *e.e.* of 96.1% and ratio of (*R*)-**1b** to (*S*)-**1b** of 98.0:2.0 (Fig. 2). Variants S237W and S237Y also displayed improved enantioselectivity of 93.0% and 92.6% *e.e.* Considering the molecular size of tryptophan and tyrosine is much larger than serine while alanine is smaller, steric hindrance is not the only factor that influences stereo recognition and binding of **1a**. Most interestingly, the enantioselectivity of S237C was significantly decreased to 27.0% *e.e.*. Variants S237M and S237I also exhibited decreased enantioselectivity of 55.5% and 44.5% *e.e.*. The hydropathy index of cysteine (2.5) was much higher than serine (− 0.8), indicating that the enantioselectivity was influenced by steric hindrance and hydrophobic interaction.

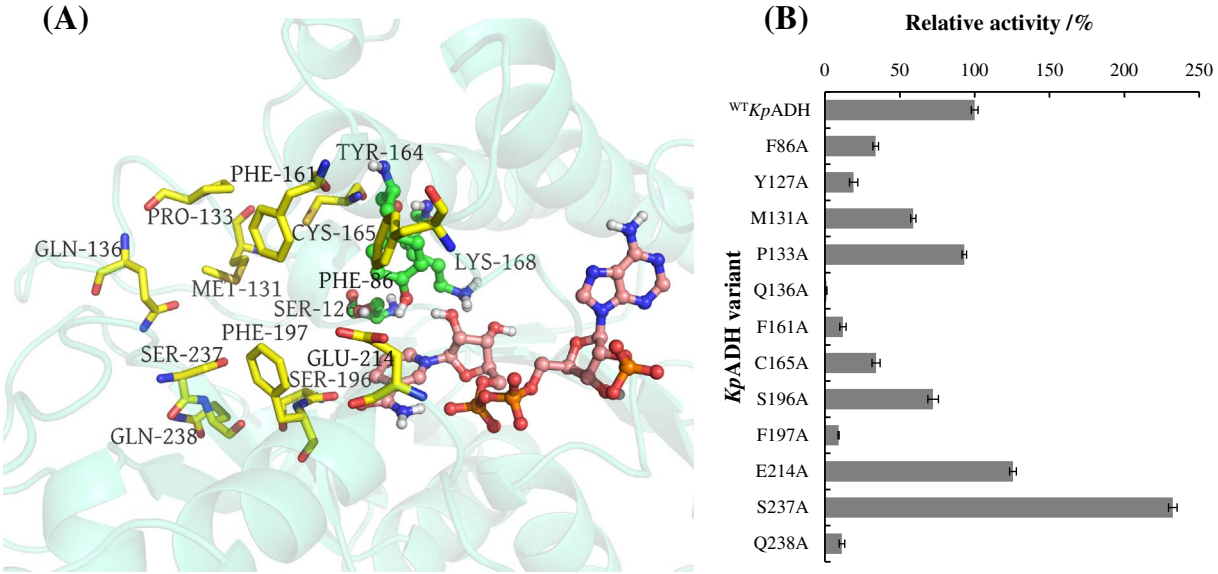

Fig. 1. Substrate binding pocket analysis of *Kp*ADH model (A) and relative activity toward **1a** of *Kp*ADH variants (B). Catalytic triad was shown in green, $NADP^+$ was depicted in pink, and residues of substrate binding pocket were shown in yellow. (For interpretation of the references to colour in this figure legend, the reader is referred to the web version of this article.)

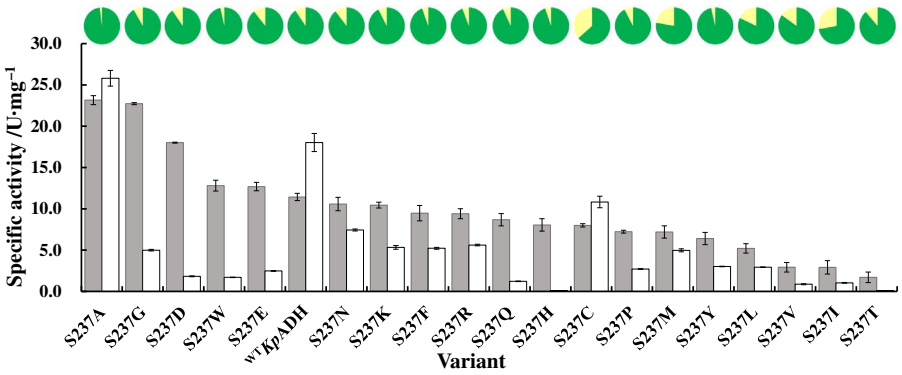

Fig. 2. Specific activity and enantioselectivity of *Kp*ADH S237 variants toward 1a. Activity was shown in bar chart (grey bar: reductive activity, white bar: oxidative activity). Enantioselectivity was illustrated in pie chart (green part: (*R*)-CPMA, yellow part: (*S*)-CPMA). Reductive activity was determined with 1.0 mM **1a** and 0.5 mM NADPH in PBS (pH 6.0, 100 mM), oxidative activity was determined with 10.0 mM isopropanol and 1.0 mM $NADP^+$ in Glycine-NaOH (pH 9.5, 100 mM) employing the standard activity assay method. (For interpretation of the references to colour in this figure legend, the reader is referred to the web version of this article.)

Table 1
Kinetic constants of *Kp*ADH variants toward **1a**.

Variant	K_m [mM]	V_{max} [μmol·min^{-1}·mg^{-1}]	k_{cat} [s^{-1}]	k_{cat}/K_m [s^{-1}·mM^{-1}]
S237G	0.62 ± 0.09	55.20 ± 3.41	36.8	59.4
S237A	0.58 ± 0.03	36.52 ± 3.02	24.4	42.1
S237H	0.45 ± 0.12	21.67 ± 2.14	14.4	32.1
S237D	0.81 ± 0.18	37.15 ± 3.28	24.8	30.6
^{WT}*Kp*ADH	0.85 ± 0.14	24.21 ± 1.95	16.1	18.9
S237W	0.76 ± 0.12	19.08 ± 2.38	12.7	16.7
S237E	0.95 ± 0.14	23.72 ± 2.95	15.8	16.6
S237R	1.16 ± 0.38	23.92 ± 1.82	16.0	13.8
S237C	1.01 ± 0.10	20.91 ± 1.82	13.9	13.8
S237N	1.04 ± 0.13	20.57 ± 0.84	13.7	13.2
S237F	0.69 ± 0.20	12.25 ± 1.50	8.17	11.8
S237K	1.12 ± 0.30	18.20 ± 0.69	12.1	10.8
S237Q	1.21 ± 0.05	17.03 ± 2.04	11.4	9.42
S237Y	0.73 ± 0.21	9.14 ± 1.31	6.09	8.34
S237M	1.06 ± 0.16	10.90 ± 0.45	7.27	6.86
S237L	1.27 ± 0.22	11.86 ± 1.09	7.91	6.23
S237P	1.36 ± 0.26	11.60 ± 1.69	7.73	5.68
S237I	0.76 ± 0.10	5.65 ± 0.43	3.77	4.96
S237V	1.28 ± 0.12	8.45 ± 0.80	5.63	4.40
S237T	0.64 ± 0.09	3.56 ± 0.56	2.37	3.70

3.3. Kinetic parameters of KpADH variants

In order to understand the binding affinity and catalytic efficiency toward **1a**, kinetic parameters were determined (Table 1). The K_m and V_{max} of ^{WT}*Kp*ADH were 0.85 mM and 24.2 μmol·min^{-1}·mg^{-1}, and the k_{cat} and k_{cat}/K_m were 16.1 s^{-1} and 18.9 s^{-1}·mM^{-1}. To the best of our knowledge, this *Kp*ADH was the most efficient alcohol dehydrogenases or carbonyl reductases in the bioreduction of **1a**. Variant S237G displayed the highest k_{cat}/K_m (59.4 s^{-1}·mM^{-1}) among all S237 variants. The K_m of S237G was 0.62 mM, 27% lower than that of ^{WT}*Kp*ADH, and the V_{max} was 55.2 μmol·min^{-1}·mg^{-1}, 2.28-fold of ^{WT}*Kp*ADH, indicating its higher binding affinity and catalytic efficiency. The k_{cat}/K_m of S237A was 42.1 s^{-1}·mM^{-1}, 2.23-fold of ^{WT}*Kp*ADH. Since glycine and alanine are the smallest amino acids, steric hindrance might be one major effect in binding and reducing of diaryl ketones, which was also proved by the decreased V_{max} of S237W, S237F and S237Y. Variants S237H and S237D also displayed improved k_{cat}/K_m, which were 32.1 and 30.6 s^{-1}·mM^{-1}. Since both histidine and aspartate are hydrophilic charged amino acids, polar interaction might be advantageous for the reduction of diaryl ketones. Mutation into other hydrophilic amino acids, such as S237E, S237R, S237K, S237N and S237Q, resulted in similar V_{max} to that of ^{WT}*Kp*ADH. Hydrophobic mutation of S237I, S237L and S237V significantly decreased the catalytic efficiency with k_{cat}/K_m of 4.96, 6.23 and 4.40 s^{-1}·mM^{-1}, ascribing to the decreased V_{max}. It is noted that the *e.e.* of S237L, S237I and S237V were also decreased to 64.1%, 44.5% and 69.8%. Increased hydrophobicity not only influenced the catalytic activity but also interfered the stereo recognition of 4-chlorophenyl and pyridin-2-yl groups. The K_m, V_{max}, and k_{cat}/K_m of S237T were 0.64 mM, 3.56 μmol·min^{-1}·mg^{-1} and 3.70 s^{-1}·mM^{-1}. S237T displayed similar binding affinity while significantly decreased catalytic efficiency due to its higher steric hindrance. The k_{cat}/K_m of S237C was 13.8 s^{-1}·mM^{-1}, little lower than ^{WT}*Kp*ADH. It is presumed that hydrophobic interaction presents stronger impact on enantioselectivity than catalytic activity. Hydrophobic interaction has been identified to be important in enantioselective recognition of prochiral ketones in alcohol dehydrogenases [22,23]. In summary, both size and hydrophilicity of residues at 237 play important roles in tuning the catalytic activity and enantioselectivity. Variants with smaller residues at 237 displayed higher activity, and variants with higher hydrophilic residues exhibited higher enantioselectivity.

Models of variants S237A, S237G and S237C were constructed based on the homology model of *Kp*ADH. **1a** was docked into each enzymes, and ten poses with the highest score were selected (Fig. S3). The calculated binding energy of ^{WT}*Kp*ADH was − 16.19 kJ·mol^{-1}, and all the poses are in favor of producing (*R*)-**1b**, with *Si*-face of **1a** orienting toward NADPH. The calculated binding energies of S237A and S237G were 0.68 and 0.31 kJ·mol^{-1} lower than ^{WT}*Kp*ADH, which provide evidence for the decreased K_m. All the poses are also located with *Si*-face orienting toward NADPH. Especially, the chlorophenyl group moves closer to A237 and G237 in all the poses. In S237C, chlorophenyl group is away from the hydrosulfuryl group of Cys237. In some poses of S237C, the *Re*-face of **1a** orients toward NADPH, leading to (*S*)-**1b**. The binding energy of S237C was calculated to be − 15.23 kJ·mol^{-1}, 0.96 kJ·mol^{-1} higher than that of ^{WT}*Kp*ADH.

3.4. Substrate profiles of KpADH variants

Substrate profiles of *Kp*ADH variants were determined against diverse prochiral ketones (Fig. 3). *Kp*ADH displayed higher activity in the asymmetric reduction of various diaryl ketones (**1a**, **7a**, **9a**) than that of aryl ketones (**2a**, **3a**, **8a**), although with apparently higher steric hindrance. *β*- and *α*-keto esters **4a** and **5a** were the "easy-to-reduce" substrates of *Kp*ADH.

Saturation mutation at S237 resulted in different substrate profiles as shown in Fig. 3. S237A and S237D displayed higher activities toward **6a** and lower toward **2a–5a** than ^{WT}*Kp*ADH. Specific activities of S237G toward **2a**, **3a** and **6a** were 1.14-, 2.43- and 1.61-fold of ^{WT}*Kp*ADH, while S237G was less efficient in reduction of **4a** and **5a** with specific activities of 67.1 and 167 U·mg^{-1}. Specific activities of S237I, S237L and S237V were lower than ^{WT}*Kp*ADH and their substrate profiles became narrower. Variants S237W, S237F and S237Y, with aromatic substituents, displayed high activity toward **1a** and **6a**. Mutation of S237 into hydrophilic amino acids, such as arginine (S237R), asparagine (S237N), glutamine (S237Q), proline (S237Q), lysine (S237K) and histidine (S237H), resulted in varied substrate profiles. Variant S237T exhibited the narrowest substrate profile, with specific activities

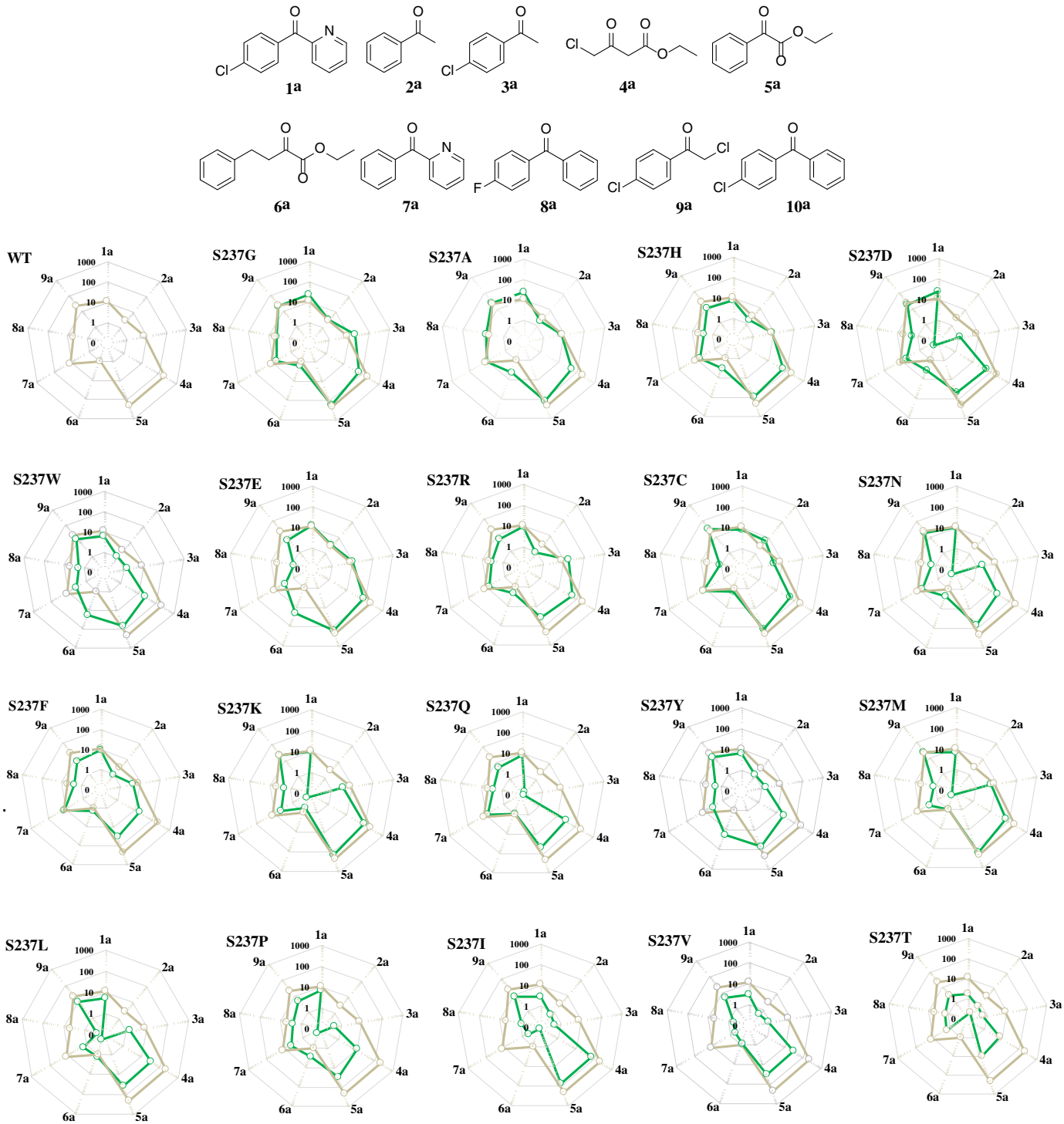

Fig. 3. Substrate spectrum of *Kp*ADH variants toward prochiral ketones. Data are shown as logarithmic in the radar map. Activities equal or lower than 0.05 U·mg^{-1} are shown as 0.05 U·mg^{-1}. The specific activities toward **10a** were not shown due to the poor solubility. Grey line: ^{WT}*Kp*ADH, green lines: *Kp*ADH variants. For detailed accounts of the numbers, see the Table S3. (For interpretation of the references to colour in this figure legend, the reader is referred to the web version of this article.)

toward **2a**–**6a** of 0.66, 0.56, 6.80, 10.0 and < 0.05 U·mg^{-1}, due to the additional methyl group of threonine. Cysteine mutation (S237C) rendered *Kp*ADH with preference toward **2a** (5.96 U·mg^{-1}), however, lower activity toward **3a**, because of the increased hydrophobicity. Variant S237G displayed the highest reducing activity toward **3a** of 19.4 U·mg^{-1}, while S237E was the most efficient in the reduction of **6a** (19.5 U·mg^{-1}). All the variants displayed decreased activities toward **7a**–**9a**, except for S237A toward **8a**. Enhanced specific activities of S237A, S237G, S237E, S237G, S237R and S237Y encouraged us to investigate their performance in the asymmetric preparation of secondary alcohols.

3.5. Asymmetric preparation of secondary alcohols employing KpADH variants

Application potential of all the beneficial variants in substrate profiles analysis was evaluated with “Substrate-coupled” cofactor regeneration mode (Table 2). Only ^{WT}*Kp*ADH, S237G and S237C

Table 2
Asymmetric reduction of **1a–10a** employing *Kp*ADH variants with isopropanol coupled cofactor regeneration.

Substrate	Conversion [%]/*e.e.* [%] (*R*/*S*)						
	^{WT}*Kp*ADH	S237A	S237C	S237E	S237G	S237R	S237Y
1a	> 99/80.8(*R*)	> 99/96.1(*R*)	> 99/27.0(*R*)	> 99/78.5(*R*)	> 99/91.6(*R*)	> 99/88.2(*R*)	> 99/92.6(*R*)
2a	> 99/89.7(*R*)	97.2/71.1(*R*)	> 99/**99.0**(*R*)	89.0/98.9(*R*)	98.5/**99.0**(*R*)	84.0/91.1(*R*)	97.5/95.5(*R*)
3a	> 99/97.5(*R*)	> 99/98.7(*R*)	98.3/**99.9**(*R*)	97.6/**99.8**(*R*)	98.6/**99.9**(*R*)	97.2/**99.6**(*R*)	98.8/**99.8**(*R*)
4a	> 99/95.3(*R*)	> 99/92.5(*R*)	> 99/92.7(*R*)	> 99/96.6(*R*)	> 99/95.9(*R*)	> 99/88.8(*R*)	98.8/90.6(*R*)
5a	88.2/73.4(*R*)	81.9/58.8(*R*)	92.7/83.2(*R*)	94.0/86.2(*R*)	97.1/93.6(*R*)	87.1/70.9(*R*)	88.8/74.5(*R*)
6a	98.2/78.0(*R*)	90.4/96.9(*R*)	> 99/64.0(*R*)	> 99/**99.0**(*R*)	> 99/64.9(*R*)	> 99/92.2(*R*)	> 99/82.6(*R*)
7a	> 99/26.5(*R*)	> 99/26.3(*R*)	> 99/38.3(*R*)	> 99/26.0(*R*)	> 99/20.0(*R*)	> 99/19.6(R)	> 99/18.1(*R*)
8a	93.2./33.6(*R*)	98.8./16.6(*R*)	88.2./59.1(*R*)	15.6/51.2(*R*)	> 99/61.7(*R*)	25.2/3.7(*R*)	22.5/26.2(*R*)
9a	> 99/95.9(*R*)	> 99/83.9(*R*)	> 99/97.3(*R*)	88.0/61.5(*R*)	> 99/6.9(*R*)	90.2/88.0(*R*)	> 99/65.4(*R*)
10a	14.4/55.3(*S*)	62.2/86.5(*S*)	7.6/36.4(*R*)	0.9/62.6(*S*)	20.5/69.7(*S*)	30.8/63.6(*S*)	1.7/81.7(*S*)

More than 99% e.e. was highlighted in bold.

displayed > 98% conversion rate in the reduction of **2a** because of their higher specific activities. It is interested to note that the *e.e.* of S237C and S237G toward **2a** was as high as 99.0%, while the *e.e.* of ^{WT}*Kp*ADH and S237A was only 89.7% and 71.1%. Substrate **3a** could be asymmetrically reduced by S237C, S237E, S237G, S237R and S237Y with > 99% *e.e.* (*R*), higher than ^{WT}*Kp*ADH (97.5%) and S237A (98.7%). All above indicates different interactions and mechanisms in the chiral recognition of diaryl ketones and aryl ketones. **4a** could be reduced into ethyl (*R*)-4-chloro-3-hydroxybutyrate, the key building block of L-carnitine [9], by all the tested variants with > 98% conversion rate, and S237E displayed the highest *e.e.* (96.6%). **5a** could be reduced into ethyl (*R*)-2-hydroxy-2-phenylacetate, which could be used for the synthesis of anticoagulant Clopidogrel [24]. Although ^{WT}*Kp*ADH displayed relatively high specific activity toward **5a**, the conversion rate and *e.e.* were only 88.2% and 73.4%. The conversion rate and *e.e.* toward **5a** of S237G were 97.1% and *e.e.* of 93.6%. **6a** could be reduced by *Kp*ADH into ethyl (*R*)-2-hydroxy-4-phenylbutyrate (**6b**), an important chiral building block for enalapril or captopril [3], with 78.0% *e.e.*, which could not satisfy the pharmaceutical requirement. It is excited to note that variant S237E could asymmetrically reduce **6a** into (*R*)-**6b** with > 99% conversion rate and 99.0% *e.e.*. Mutation at residue S237 also influenced the enantioselectivity of *Kp*ADH in the reduction of **7a–10a** (Table 2). The *e.e.* of S237C, S237G and S237A toward **7a**, **8a** and **10a** increased to 38.3%, 61.7% and 86.5% from 26.5%, 33.6% and 55.3% of ^{WT}*Kp*ADH. All above demonstrates the importance of residue S237 in tuning the activity and enantioselectivity of *Kp*ADH for the asymmetric preparation of chiral secondary alcohols.

4. Conclusions

In summary, residue Ser237 was identified to be important in fine tuning the activity and enantioselectivity of *Kp*ADH. The *e.e.* of S237A toward (4-chlorophenyl)-(pyridin-2-yl)-methanone improved to 96.1%, while the *e.e.* of S237C decreased to 27.0% in comparison with 82.0% *e.e.* of ^{WT}*Kp*ADH. All the variants exhibited different substrate profiles from ^{WT}*Kp*ADH. Variants S237C, S237G and S237E could catalyze the asymmetric reduction of acetophenone, 4-chloroacetophenone and ethyl 2-oxo-4-phenylbutyrate with > 99% *e.e.*. Both steric hindrance and hydrophilicity are key factors in manipulating the substrate specificity and enantioselectivity of *Kp*ADH.

Acknowledgements

We are grateful to the National Natural Science Foundation of China (21506073, 21776112), the Natural Science Foundation of Jiangsu Province (BK20150003, BK20171135), Six talent peaks project of Jiangsu Province (2015-SWYY-008), the Program of Introducing Talents of Discipline to Universities (111-2-06), and a project funded by the Priority Academic Program Development of Jiangsu Higher Education Institutions for the financial support of this research.

Appendix A. Supplementary data

Supplementary data to this article can be found online at https://doi.org/10.1016/j.catcom.2018.01.012.

References

[1] F. Hollmann, I.W.C.E. Arends, D. Holtmann, Enzymatic reduction for the chemist, Green Chem. 13 (2011) 2285–2314.
[2] K. Nakamura, R. Yamanaka, T. Matsuda, T. Harada, Recent developments in asymmetric reduction of ketones with biocatalysts, Tetrahedron Asymmetry 14 (2003) 2659–2681.
[3] G.C. Xu, Y. Ni, Bioreductive preparation of ACE inhibitors precursor (*R*)-2-hydroxy-4-phenylbutanoate esters: recent advances and future perspective, Bioresour. Bioproces. 2 (2015) e15.
[4] J.H. Tao, J.H. Xu, Biocatalysis in development of green pharmaceutical processes, Curr. Opin. Chem. Biol. 13 (2009) 43–50.
[5] J.C. Morre, D.J. Pollard, B. Kosjek, P.N. Devine, Advances in the enzymatic reduction of ketones, Acc. Chem. Res. 40 (2007) 1412–1419.
[6] T. Matsuda, R. Yamanaka, K. Nakamura, Recent progress in biocatalysis for asymmetric oxidation and reduction, Tetrahedron Asymmetry 20 (2009) 513–557.
[7] C. Filling, K.D. Berndt, J. Benach, S. Knapp, T. Prozorovski, E. Nordling, R. Ladenstein, H. Jörnvall, U. Oppermann, Critical residues for structure and catalysis in short-chain dehydrogenase/reductases, J. Biol. Chem. 227 (2002) 25677–25684.
[8] S. Luetz, L. Giver, J. Lalonde, Engineered enzymes for chemical production, Biotechnol. Bioeng. 101 (2008) 647–653.
[9] G.C. Xu, H.L. Yu, Y.P. Shang, J.H. Xu, Enantioselective bioreductive preparation of chiral halohydrins employing two newly identified stereocomplementary reductases, RSC Adv. 5 (2015) 22703–22711.
[10] N. Itoh, K. Isotani, M. Nakamura, K. Inoue, Y. Isogai, Y. Makino, Efficient synthesis of optically pure alcohols by asymmetric hydrogen-transfer biocatalysis: application of engineered enzyme in a 2-propanol-water medium, Appl. Microbiol. Biotechnol. 93 (2012) 1075–1085.
[11] I. Lavandera, A. Kern, B. Ferreira-Silva, A. Glieder, S. de Wildeman, W. Kroutil, Stereoselective bioreduction of bulky-bulky ketones by a novel ADH from *Ralstonia* sp, J. Org. Chem. 73 (2008) 6003–6005.
[12] Y. Ni, J.H. Xu, Biocatalytic ketone reduction: a green and efficient access to enantiopure alcohols, Biotechnol. Adv. 30 (2012) 1279–1288.
[13] E.J. Corey, C.J. Helal, Asymmetric synthesis of (S)-carbinoxamine. New aspects of oxazaborolidine-catalyzed enantioselective carbonyl reduction, Tetrahedron Lett. 37 (1996) 5675–5678.
[14] M. Shimizu, T. Fujisawa, A new approach to optically active 1,2-diaryl-1,2-diaminoethanes and 1,2-diaryl-2-aminoethanols, J. Syn. Org. Chem. JPN 56 (1998) 672–680.
[15] C.Y. Chen, R.A. Reamer, J.R. Chilenski, C.J. McWilliams, Highly enantioselective hydrogenation of aromatic-heteroaromatic ketones, Org. Lett. 5 (2003) 50392–55042.
[16] M.D. Truppo, D. Pollard, P. Devine, Enzyme-catalyzed enantioselective diaryl ketone reductions, Org. Lett. 9 (2007) 335–338.
[17] H.M. Li, D.M. Zhu, L. Hua, E.R. Biehl, Enantioselective reduction of diaryl ketones catalyzed by a carbonyl reductase from *Sporobolomyces salmonicolor* and it mutant enzymes, Adv. Synth. Catal. 351 (2009) 583–588.
[18] Y. Ni, J.Y. Zhou, Z.H. Sun, Production of a key chiral intermediate of Betahistine with a newly isolated *Kluyveromyces* sp. in an aqueous two-phase system, Process Biochem. 47 (2012) 1042–1048.
[19] J.Y. Zhou, G.C. Xu, R.Z. Han, J.J. Dong, W.G. Zhang, R.Z. Zhang, Y. Ni, Carbonyl group-dependent high-throughput screening and enzymatic characterization of diaromatic ketone reductase, Catal. Sci. Technol. 6 (2016) 6320–6327.

[20] P.C. Guo, Z.Z. Bao, X.X. Ma, Q.Y. Xia, W.F. Li, Structural insights into the cofactor-assisted substrate recognition of yeast methylglyoxal/isovaleraldehyde reductase Gre2, Biochim. Biophy. Acta 1844 (2014) 1486–1492.
[21] J. Cheng, G.C. Xu, R.Z. Han, J.J. Dong, Y. Ni, Efficient access to L-phenylglycine using a newly identified amino acid dehydrogenase from *Bacillus clausii*, RSC Adv. 6 (2016) 80557–80563.
[22] D.M. Zhu, Y. Yang, S. Majkowicz, T.H.Y. Pan, K. Kantardjieff, L. Hua, Inverting the enantioselectivity of a carbonyl reductase via substrate-enzyme docking-guided point mutation, Org. Lett. 10 (2008) 525–528.
[23] M.M. Musa, N. Lott, M. Laivenieks, L. Watanabe, C. Vieille, R.S. Phillips, A single point mutation reverses the enantiopreference of *Themoanaerobacter ethanolicus* secondary alcohol dehydrogenase, ChemCatChem 1 (2009) 89–93.
[24] H.M. Ma, L.L. Yang, Y. Ni, J. Zhang, C.X. Li, G.W. Zheng, H.Y. Yang, J.H. Xu, Stereospecific reduction of methyl *o*-chlorobenzoylformate at 300 g L^{-1} without additional cofactor using a carbonyl reductase mined from *Candida glabrata*, Adv. Synth. Catal. 354 (2012) 1765–1772.